Physics Letters B 709 (2012) 59–64

Contents lists available at SciVerse ScienceDirect

Physics Letters B

www.elsevier.com/locate/physletb

Long-lived three-quasiparticle isomers in ^{191}Ir and ^{193}Ir with triaxial deformation

G.D. Dracoulis [a,*], G.J. Lane [a], A.P. Byrne [a], H. Watanabe [a,b], R.O. Hughes [a,1], N. Palalani [a], F.G. Kondev [c], M. Carpenter [d], R.V.F. Janssens [d], T. Lauritsen [d], C.J. Lister [d], D. Seweryniak [d], S. Zhu [d], P. Chowdhury [e], Y. Shi [f], F.R. Xu [f]

[a] Department of Nuclear Physics, R.S.P.E., Australian National University, Canberra, A.C.T. 0200, Australia
[b] RIKEN Nishina Center, 2-1 Hirosawa, Wako, Saitama 351-0198, Japan
[c] Nuclear Engineering Division, Argonne National Laboratory, Argonne IL, USA
[d] Physics Division, Argonne National Laboratory, Argonne IL, USA
[e] Department of Physics, University of Massachusetts Lowell, Lowell, MA 01854, USA
[f] School of Physics, Peking University, Beijing 100871, China

ARTICLE INFO

Article history:
Received 27 December 2011
Received in revised form 2 February 2012
Accepted 3 February 2012
Available online 7 February 2012
Editor: D.F. Geesaman

ABSTRACT

Deep-inelastic reactions have been used to populate high-spin states in the iridium isotopes. New results include the identification of particularly long-lived three-quasiparticle isomers in ^{191}Ir and ^{193}Ir, with mean-lives of 8.2(7) s and 180(3) μs respectively, decaying into newly identified states of the $h_{11/2}$ proton bands and into other structures. Spins and parities of $J^{\pi} = 31/2^{+}$ are suggested for both, consistent with coupling of the $11/2^{-}[505]$ proton to the 10^{-} two-neutron excitations in the cores. These and other configurations are discussed in the context of configuration constrained potential-energy-surface calculations. All calculated intrinsic states are expected to be associated with triaxial shapes and the extreme isomerism observed is attributed to spin-trapping rather than K-hindrance.

The iridium isotopes ($Z = 77$) near the stability line fall at the perimeter of the region of well-deformed nuclei. Together with the neighboring isotopes of osmium ($Z = 76$) and platinum ($Z = 78$), they constitute a group that is of considerable interest in terms of nuclear structure. This is partly because these nuclei are expected to exhibit increasing gamma-softness [1,2], shape evolution [3–8], and a predicted configuration-dependence and susceptibility to dynamic (rotation-induced) shape changes [9–11].

An implicit assumption of the move away from a well-defined deformation with axial symmetry is that K, the quantum number describing the projection of the total angular momentum on the deformation axis, will not be conserved. The inhibition of nominally forbidden γ-ray decays will thus be reduced, resulting in relatively shorter lifetimes and fewer isomers [12–14]. This anticipated dilution of the K-quantum number due to dynamical effects and the absence of a single deformation axis, is challenging to treat quantitatively [15,16]. Nevertheless, the (perceived) absence of K-isomers is regularly taken as an indication of γ-softness (see [17]). Shell-model-type isomers are expected, of course, as shell closures are approached, and precursors to these are observed as relatively short-lived isomers in the nearby platinum and mercury isotopes, ^{194}Pt [18] and ^{196}Hg [19].

The focus of the present work was the discovery and characterization of isomeric states in the stable isotopes ^{191}Ir and ^{193}Ir, with the aim of elucidating the transitional character of the nuclear structure in this region. Their stability, however, meant that they could not be accessed with conventional nuclear reactions such as heavy-ion induced, fusion-evaporation. Much of the previous information has thus come from Coulomb excitation and β-decay studies, both of which are limited in terms of the states that can be populated. Our studies draw on the demonstrated ability of so-called "deep inelastic" heavy-ion reactions to populate high-spin states in a broad range of nuclei through either inelastic excitation, or transfer of a few particles between a particular projectile and target nucleus [20]. The experimental configuration of thick-target, stopped measurements is more effective for the population and identification of states that are either long-lived, or are fed by isomers, than for the identification of very short-lived states (ps range) that is limited by Doppler broadening.

Surprisingly, long-lived isomers were found despite their association with triaxial configurations. As will be discussed in due course, the isomerism apparently results because these configurations form spin-traps, rather than because their decays are K-inhibited.

* Corresponding author.
E-mail address: george.dracoulis@anu.edu.au (G.D. Dracoulis).
[1] Present address: Department of Physics, University of Richmond, 28 Westhampton Way, Richmond, VA 23173, USA.

0370-2693/$ – see front matter
doi:10.1016/j.physletb.2012.02.008

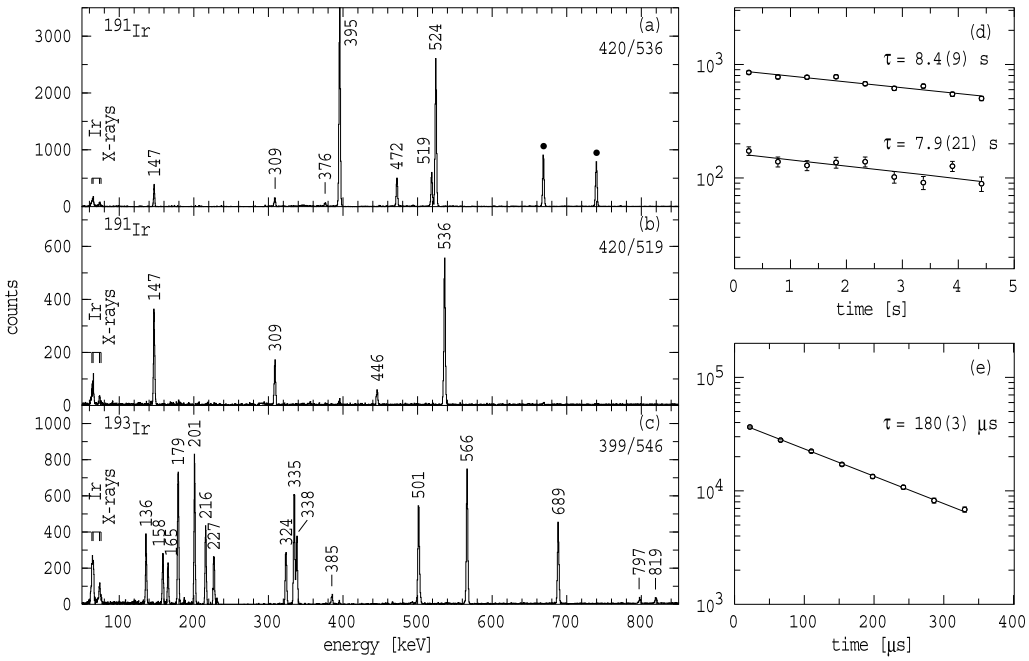

Fig. 1. Out-of-beam γ-ray spectra with double γ-ray coincidence gates in ^{191}Ir (panels (a) and (b)) and in ^{193}Ir (panel (c)). In these, known contaminants are indicated by filled circles. Panel (d) gives the decay curves for the two paths in ^{191}Ir (the weaker one being via the 309 keV transition) and panel (e) is a representative decay curve for the isomer in ^{193}Ir, as discussed in the text.

The measurements used 6.0 MeV/u ^{136}Xe beams provided by the ATLAS facility at Argonne National Laboratory. Nanosecond pulses, separated by 825 ns, were incident on three targets, enriched metallic ^{186}W and ^{187}Re foils, ~ 6 mg/cm^2 thick with 25 mg/cm^2 gold foil directly behind them and a pressed 44 mg/cm^2 enriched ^{192}Os target with a 10 mg/cm^2 gold foil behind. Gamma rays were detected by Gammasphere [21], with 100 detectors in operation. Triple coincidence events were required and the main data analysis was carried out with γ–γ–γ cubes, using various time-difference conditions, and also with time constraints relative to the pulsed beam, allowing selection of different out-of-beam regimes.

Another set of measurements was carried out using a macroscopically chopped beam with various (beam on)/(beam off) conditions. In these, out-of-beam dual coincidence events were recorded in reference to a precision clock and γ–γ matrices as a function of time were constructed in contiguous time regions, allowing long lifetimes to be isolated by gating on specific cascades within the nucleus of interest. Scans were made with different conditions, progressing in steps of ten, from initial values in the sub-millisecond range up to the region of a few seconds, the maximum that could be accommodated by the electronics. The scans of most relevance here are the set with the ^{186}W target covering a complete range from 10/40 μs, in steps of ten up to 1/4 s, and also two measurements with the ^{192}Os target and 100/400 μs and 1/4 ms ranges. Results for the neutron-rich isotopes ^{188}W and ^{190}W from the same set of measurements were reported recently [22] and studies of ^{190}Os, ^{192}Os and ^{194}Os have also been completed [23,24].

The assignment of γ rays to specific isotopes depends partly on prior knowledge of some transitions between low-lying states, complemented by coincidences with the characteristic X rays that follow internal conversion. An independent guide to isotopic assignment comes through evaluation of relative yields with the same or different targets, each additional particle transfer usually leading to about an order of magnitude lower population. While spectroscopic information is often limited in such measurements, in the present work, total conversion coefficients deduced from (delayed) intensity balances and γ–γ angular correlations were used, together with the usual considerations of γ-ray branching and transition strengths, to constrain spin and parity assignments. (See Ref. [25] for examples of the angular correlation technique.)

New results are reported here for ^{191}Ir and ^{193}Ir. Previously in ^{191}Ir, delayed feeding from an unidentified isomer, indirectly populating states in the rotational band based on the $h_{11/2}$ proton (the $11/2^-[505]$ Nilsson orbital) had been reported from studies using the ^{192}Os(d, 3n)^{191}Ir reaction [26]. The $h_{11/2}$ band had also been identified in ^{193}Ir [11], but no isomers were known.

Selected spectra obtained with double gates on delayed transitions in ^{191}Ir and ^{193}Ir are given in Fig. 1. The main delayed transitions feeding the $19/2^-$ state of the $11/2^-$ band in ^{191}Ir, are evident in Fig. 1(a), the stronger path being from the cascade of 536-keV and 395-keV transitions located directly above. This was the path identified previously [26], with a delayed component attributed to an unobserved transition from a long-lived isomer with $T_{1/2} = 5.5(7)$ s, corresponding to a meanlife of 7.9(10) s, feeding a state at 2047 keV.

The partial level scheme deduced for ^{191}Ir from the present work is given in Fig. 2.

Our angular correlation results show that the 395-keV transition is a mixed dipole, and therefore probably of $E2/M1$ character. Together with the total conversion coefficient of 0.11(2) (see Fig. 3), this leads to a $J^\pi = 25/2^-$ assignment for the 2047-keV state. Although it could be a candidate for the $25/2^-$ member of the $11/2^-[505]$ band, we do not observe the expected, but possibly weak, $E2$ branch to the $21/2^-$ member (see below), and the sign of the A_2 coefficient in the angular correlation obtained by gating on stretched quadrupole transitions lower in the scheme is opposite to those of the measured correlations for the 472-keV and 446-keV transitions (see Fig. 2) obtained in an equivalent way. Although, at face value, these properties are not consistent with the 395-keV transition being a band member, there is an alignment in this region and, therefore, a change in structure that could alter the sign of the mixing ratio is possible.

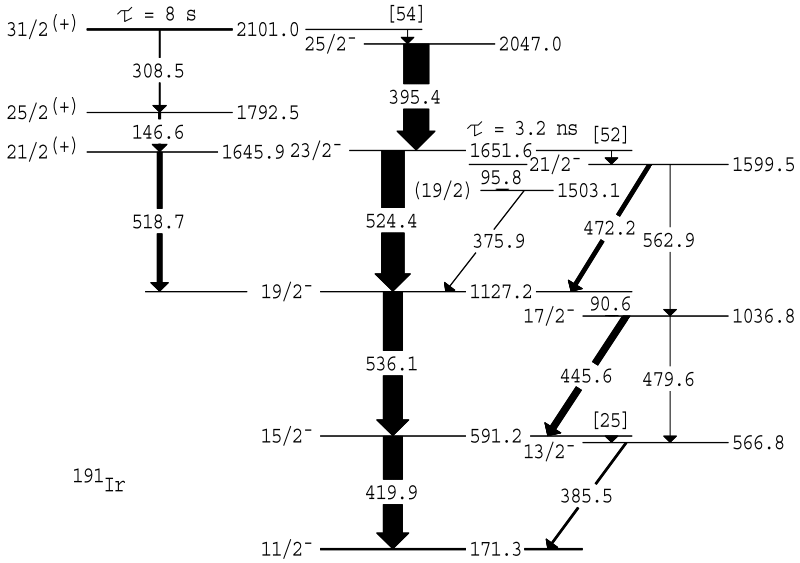

Fig. 2. Partial level scheme for ^{191}Ir, including the main decays from the isomer and the $h_{11/2}$ band. Unobserved low-energy transitions implied by the γ–γ coincidences are indicated by square brackets.

While our results confirm the main transitions and the $13/2^-$, $17/2^-$ states in the unfavored signature sequence, an additional delayed path is evident from the coincidence spectra given in Fig. 1(a) and 1(b). The sequence of 308.5-, 146.6- and 518.7-keV transitions constitutes a parallel cascade, feeding through the $19/2^-$, 1128-keV level, implying a state at 2101 keV, 54 keV above the 2047-keV, $25/2^-$ state in the main cascade. (The ordering of the 146.6-keV and 308.5-keV transitions is unambiguous since only the former is promptly fed.) Our contention is that the 2101 keV level is the isomeric state, with an unobserved (presumably highly converted) 54-keV transition to the 2047 keV state. This is consistent with the observation of both prompt and delayed feeding of the 2047 keV state in the earlier work.

The 518.7-keV transition was also known from the (d, 3n) studies and assigned as a decay from a 1646 keV state. This level was suggested to be the $21/2^-$ member of the unfavored sequence of the $h_{11/2}$ band [26]. However, we propose a new state at 1599.6 keV as the $21/2^-$ member, consistent with its decays to other band members, the mixed dipole/quadrupole character of the 472.2-keV transition to the $19/2^-$ state (similar in character to the 445.6- and 385.5-keV transitions) and the feeding via an unobserved low-energy transition from the 1652-keV, $23/2^-$ state. In contrast, the present angular correlation results indicate that the 518.7-keV γ-ray is essentially a pure stretched dipole transition ($\delta < 0.05$), as was also found in the (d, 3n) study, in conflict with the expectation from the triaxial rotor model calculations reported in Ref. [26] that predicted a mixed transition with $\delta = 0.18$. These considerations and the absence of other branches, such as a possible $21/2^- \rightarrow 17/2^-$ transition in the case of negative parity (as is observed in ^{193}Ir — see below) leads to the proposed $21/2^{(+)}$ assignment for the 1646-keV state.

Two additional pieces of evidence for parallel paths from a single isomer are (i) that the measured lifetimes from both paths agree as evidenced by the data and fits given in Fig. 1(d) (although the weaker path is not as accurately determined) and both are consistent with the value obtained from the (d, 3n) measurements [26]; and (ii) that the 309-keV transition placed as a decay directly from the isomer is strongly converted (Fig. 3), indicating a high multipolarity ($M3$) and, therefore, the expectation of a long lifetime. The angular correlation and total conversion results for the 146.6- and 308.5-keV transitions then lead to the probable

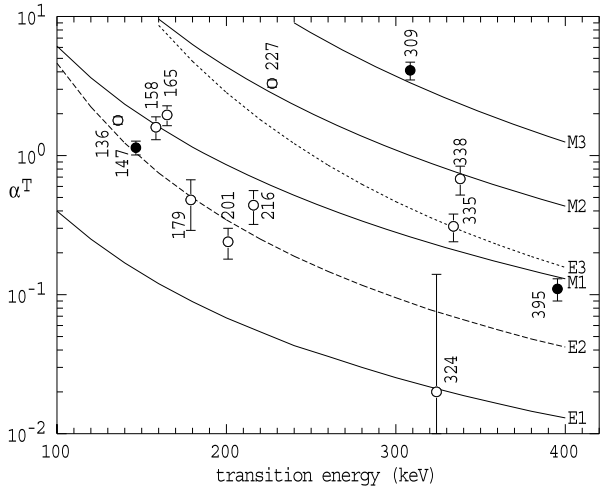

Fig. 3. Total conversion coefficients deduced from various intensity balances in ^{191}Ir (filled symbols) and ^{193}Ir (open symbols) compared with predicted values.

$31/2^+$ assignment for the isomer. (The residual uncertainty in the parity reflects the fact that the positive parity assignment to the 1646 keV state is favored but not definitive.) With the present assignment, the (unobserved) 54-keV transition to the 2047-keV, $25/2^-$ state would be of $E3$ character. The corresponding transition strengths are given in Table 1.

The $E3$ and $M3$ branches in ^{191}Ir are hindered by factors of 100 and 1000 with respect to single-particle values. These hindrances are not particularly large, although to interpret them in terms of K-forbiddenness it is necessary to know the K-values of the final states. It is not clear whether these are collective states of relatively low-K, or intrinsic states with (nominally) high-K values. For example, if the $25/2^-$ state at 2047-keV is assumed to have (mainly) $K = 11/2$, the reduced hindrance, $f_\nu = \Delta K - \lambda$, of the 54-keV $E3$ transition for $\nu = 7$, is only 1.8, effectively unhindered. This value is lower even than the $E3$ decays to the γ band from the $K^\pi = 10^-$ isomer in ^{192}Os, which have $f_\nu \sim 5$ (see [24] for a recent evaluation) and is consistent with the trend of low hindrances seen in the heavy tungsten isotopes [22].

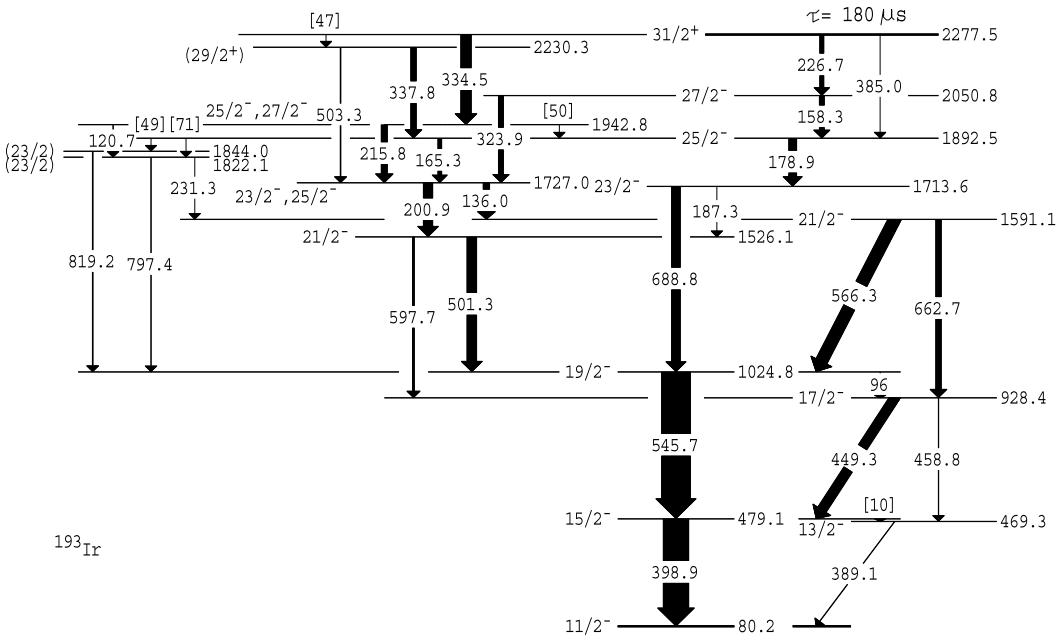

Fig. 4. Partial level scheme for ^{193}Ir. Unobserved low-energy transitions are indicated by square brackets.

Table 1
Transition strengths and hindrances for the long-lived isomers in ^{191}Ir and ^{193}Ir.

E_γ (keV)	I_γ rel.	Final state	$\sigma\lambda$	α_T[a]	Strength (W.u.)
^{191}Ir [$E = 2101$ keV; $K^\pi = 31/2^+$; $\tau = 8.2(7)$ s]					
54.0	2.20(2)[b]	$25/2^-$	$E3$	3800	$1.62(14) \times 10^{-2}$
308.5	380(18)	$25/2^+$	$M3$	3.34	$1.52(15) \times 10^{-3}$
^{193}Ir [$E = 2278$ keV; $K^\pi = 31/2^+$; $\tau = 180(3)$ μs]					
47.2	406(12)[b]	$(29/2^+)$	$(M1)$	9.65	$4.1(2) \times 10^{-8}$
334.5	4153(57)	$(25/2^-)$[c]	$(E3)$[c]	0.303	2.33(6)
226.7	1715(51)	$27/2^-$	$M2$	2.81	$1.27(5) \times 10^{-3}$
385.0	389(44)	$25/2^-$	$E3$	0.179	$8.1(9) \times 10^{-2}$

[a] Ref. [27].
[b] γ-Ray intensity inferred from total intensity balance.
[c] The alternative $M2$ transition in the case of a $27/2^-$ assignment to the 1943 keV state would have a strength of about 4×10^{-4} W.u.

Other isomers were searched for by projecting intermediate-time spectra with γ-ray gates above and below each state of interest. This technique is sensitive down to a region of about 1 ns for strong lines in the present experiment. The only significant finding was the lifetime of $\tau = 3.2(5)$ ns assigned to the 1652-keV level.

The level scheme deduced for ^{193}Ir is given in Fig. 4. The $h_{11/2}$ band was recently extended up to a proposed $23/2^-$ state at 1714 keV in studies using incomplete fusion reactions [11], but no isomers were identified. We confirm the earlier work, but observe strong delayed population with a complex path, originating from a long-lived state at 2278 keV. The main transitions are evident in Fig. 1(c). Four de-excitation pathways from the isomer have been established with primary decays of 226.7-, 385.0-, 334.5- and an unobserved 47-keV transition. Transition strengths are given in Table 1 While the uppermost isomer has a meanlife of 180(3) μs, evidence for which is found in Fig. 1(e), surprisingly perhaps, none of the lower states have significant lifetimes. A conservative limit of $\leqslant 2$ ns can be placed on these. Such short lifetimes imply that essentially none of the γ rays observed can have a significant proportion of $M2$ (or higher) multipolarity, hence mixed dipole transitions must be of $E2/M1$ character.

Previous spectroscopic information on the $11/2^-$ band was limited, but from the γ–γ correlation measurements we can confirm the stretched quadrupole character of the 546- and 689-keV transitions, and mixed ($E2/M1$) character for the 566- and 449-keV decays from states in the unfavored signature sequence. The 501-keV γ-ray from the 1526 keV state is also a mixed dipole transition, with a weaker (presumably $E2$) branch to the $17/2^-$ state, consistent with the $21/2^-$ assignment to the 1526 keV level. The 1727-keV state has a 136-keV decay to the 1591-keV, $21/2^-$ state with a conversion coefficient suggesting a mixed $E2/M1$ transition and a 201-keV decay to the 1526 keV, $21/2^-$ level. Although the conversion coefficient for the 201-keV transition is close to a pure $E2$ value, its angular correlation is difficult to characterize definitively, hence the possible $23/2^-$ or $25/2^-$ assignment for the 1727-keV level (Fig. 4).

The 1727-keV state is fed by a 165-keV transition with a conversion coefficient characteristic of an $M1$ multipolarity, suggesting $J^\pi = 25/2^-$ for the 1893-keV level. This state's main decay is via the 179-keV transition to the 1714-keV, $23/2^-$ level. The 179-keV γ-ray was assigned as a stretched quadrupole in Ref. [11] on the basis of a (marginal) *DCO* ratio and the total conversion coefficient from the present delayed intensity balances suggests a dominant $E2$ multipolarity. However, the angular correlation is inconsistent with a stretched quadrupole nature, but it is consistent with a $\Delta J = 1$ transition with either a small, or a large mixing ratio, the latter of which ($\delta(E2/M1) \sim 14$) corresponds to essentially pure $E2$ character, evidence again for the $25/2^-$ assignment to the 1893-keV state.

Directly above the 1893-keV level, the 158.3-keV γ-ray is assigned as a stretched $M1$ transition,while the 226.7-keV decay from the isomer has a large conversion coefficient consistent with an $M2$ character (see Fig. 3). This leads to the proposed $J^\pi = 31/2^+$ assignment for the 2277.5-keV isomeric state. The spectroscopic information from the other main decay path, considering both the angular correlation and total conversion data (Fig. 3), is less certain because the extraction of total conversion coefficients is complicated by multiple branches and the fact that the transitions below (such as the 501- and 566-keV γ-rays) are mixed dipoles, introducing more

Table 2
Selected three-quasiparticle configurations in ^{191}Ir and ^{193}Ir together with calculated energies and deformations.

K^π	Configuration	^{191}Ir				^{193}Ir			
		β_2	γ (deg.)	β_4	$E^{cal.}$ (keV)	β_2	γ (deg.)	β_4	$E^{cal.}$ (keV)
$21/2^-$	$\nu 11/2^+[615]$, $7/2^-[503] \otimes \pi 3/2^+[402]$	0.149	19	−0.048	1938	0.141	18	−0.055	2635
$23/2^+$	$\nu 11/2^+[615]$, $1/2^-[510] \otimes \pi 11/2^-[505]$	0.147	36	−0.024	2008	0.131	30	−0.023	2289
$23/2^-$	$\nu 11/2^+[615]$, $9/2^-[505] \otimes \pi 3/2^+[402]$	0.157	24	−0.044	2014	0.138	18	−0.039	2435
$25/2^+$	$\nu 11/2^+[615]$, $3/2^-[512] \otimes \pi 11/2^-[505]$	0.147	22	−0.045	2140	0.148	30	−0.077	2487
$27/2^+$	$\nu 11/2^+[615]$, $13/2^+[606] \otimes \pi 3/2^+[402]$	0.147	33	−0.034	2536	0.137	33	−0.037	2060
$29/2^+$	$\nu 11/2^+[615]$, $7/2^-[503] \otimes \pi 11/2^-[505]$	0.149	24	−0.035	2511	0.138	26	−0.034	2860
$31/2^-$	$\nu 9/2^+[624]$, $11/2^+[615] \otimes \pi 11/2^-[505]$	0.147	32	−0.026	2086	0.130	25	−0.050	2460
$31/2^+$	$\nu 11/2^+[615]$, $9/2^-[505] \otimes \pi 11/2^-[505]$	0.157	27	−0.040	2210	0.135	14	−0.039	2583
$33/2^-$	$\nu 11/2^+[615]$, $13/2^+[606] \otimes \pi 9/2^-[514]$	0.155	39	−0.026	2853	0.138	34	−0.027	2432
$35/2^-$	$\nu 11/2^+[615]$, $13/2^+[606] \otimes \pi 11/2^-[505]$	0.145	33	−0.043	2639	0.134	33	−0.046	2119

ambiguity into the correlation analysis. Nevertheless, the suggested mixed $E2/M1$ character for the 215.7-keV transition from both the correlation and the total conversion coefficient leads to $25/2^-$ or $27/2^-$ for the 1943-keV state, dependent on the spin choice for the lower 1727-keV state. The conversion coefficient (Fig. 3) of the 334.5-keV transition feeding the 1943-keV level is close to the calculated $E3$ value although the resultant $E3$ strength of about 2 W.u. (Table 1) implies specific configuration changes that are not expected on the basis of the available orbitals.

The two main decay paths are also connected via the 323.9-keV transition from the 2051-keV, $27/2^-$ state to the 1727-keV, $23/2^-$ level. Its conversion coefficient is not precisely determined (due mainly to contaminant issues), but is consistent with an $E2$ character.

The 2230.3-keV state, whose main decay proceeds via the 337.8-keV transition to the 1893-keV, $25/2^-$ level, is shown as being fed by an unobserved 47-keV transition from the 180-μs isomer. This is consistent with the fact that some prompt population is observed for this state. However, we cannot discount the possibility that the 2230-keV state also has a lifetime (given the $M2$ character suggested by the conversion coefficient), although it would have to be in the intermediate range of a few microseconds for it not to have been evident in either the pulsed data, or in the long-chopping experiment.

Turning now to the nuclear structure of these long-lived states, multi-quasiparticle calculations, carried out with fixed deformations, normally provide a reasonable guide to the intrinsic states that might give rise to isomers. However, in the present case, configuration-dependent deformations that differ significantly from those associated with the one-quasiparticle configurations are likely to occur. Of direct interest here, for example, is the predicted $31/2^+$ state obtained by coupling the $11/2^-[505]$ proton to the 10^-, two-quasineutron isomers found at 1705 keV in ^{190}Os and 2015 keV in ^{192}Os. The proton configuration is known to favor a triaxial deformation (as evidenced by the large signature splitting in its rotational band), whereas the 10^- configuration is predicted to be essentially prolate [10]. (Note that the predicted ground-state deformations calculated by Moller et al. [28] do not specify the configuration.)

To address these issues, calculations allowing for self-consistent shape changes were carried out for a range of odd-A iridium isotopes. The most likely 3-quasiparticle configurations were computed using the method of K-constrained diabatic potential-energy surfaces [29,30] with a non-axial deformed Woods–Saxon potential and approximate particle-number projection achieved through the Lipkin–Nogami prescription. The results for selected states (mainly the highest-spin, lowest-energy states predicted) are listed in Table 2.

Key high-spin states involve the coupling of a proton to either the (core) 10^- states from the $11/2^+[615]$, $9/2^-[505]$ two-neutron configuration, or the 10^+ and 12^+ states formed from a pair of $i_{13/2}$ neutron orbitals, specifically the $9/2^+[624]$, $11/2^+[615]$ and $11/2^+[615]$, $13/2^+[606]$ configurations. The predicted energy of the 12^+ configuration is predicted to drop rapidly with neutron number, hence, the $35/2^-$ state obtained by adding to it the $11/2^-[505]$ proton is expected to be significantly lower in energy than the predicted $31/2^+$ and $31/2^-$ levels in ^{193}Ir. This may be somewhat artificial since there is minimal experimental information on single-particle levels in this region. Related predictions of low-lying 12^+ isomers in the osmium isotopes have yet to be borne out [22]. Alternatively, a very low energy could result in long-lived states that would preferentially β decay, and thus be missed.

As can be seen from Table 2, both $31/2^-$ and $31/2^+$ intrinsic states are predicted, fairly close to the excitation energies of the observed isomers. Although the calculations place the $31/2^-$ level lower in both isotopes, they do not include the residual interactions that favor the $31/2^+$ configuration. With an experimental assignment of $31/2^+$, an association in both nuclei with the predicted $31/2^+$ configuration is natural, but a $31/2^-$ state should also be expected.

All of the states predicted are associated with significant triaxiality, even in the cases which involve the 10^- two-neutron component that is calculated to be symmetric in the even–even cores [10]. This presumably reflects the shape-driving effect of the additional proton. There are no obvious theoretical candidates to match the $25/2^-$ and $27/2^-$ states observed near 2 MeV. These are probably collective excitations (consistent also with the absence of significant lifetimes) which will be numerous because of the triaxiality. Two other types of structure which may be present are negative parity states associated with the $11/2^-[505]$ configuration and alignment of the $h_{9/2}$ protons, and corresponding levels arising from rotation alignment of the $i_{13/2}$ neutrons at *oblate* deformation analogous to those predicted for the even–even neighbors [10] and observed (near 2.8 MeV) in ^{192}Os [23].

While the transition strengths cannot be evaluated in detail because of the uncertainty in the final configurations, it seems that the long-lived isomers occur largely because the decays proceed by relatively low-energy, high-multipolarity transitions rather than because of significant K-hindrance. They are in effect spin-traps rather than K-isomers [13]. In this regard, the absence of any other isomers in the decay path, particularly in ^{193}Ir, is also pertinent as a possible indication of the absence of K-hindrance. The calculations also indicate that even longer-lived β-decaying isomers should occur, providing a challenge for future studies and in effect, a test of the reliability of the models.

Acknowledgements

We are grateful to R.B. Turkentine for preparing the targets. This work was supported by the Australian Research Council grants DP0986725, DP03445844 and FT100100991, and the U.S. Department of Energy, Office of Nuclear Physics, under Contract No. DE-AC02-06CH11357 and Grant No. DE-FG02-94ER40848.

References

[1] C.Y. Wu, et al., Nucl. Phys. A 607 (1996) 178.
[2] C.Y. Wu, D. Cline, Phys. Rev. 54 (1996) 2356.
[3] C. Wheldon, et al., Phys. Rev. C 63 (2001) 011304.
[4] L.M. Robledo, R. Rodriguez-Guzman, P. Sarriguren, J. Phys. G 36 (2009) 115104.
[5] P. Sarriguren, R. Rodriguez-Guzman, L.M. Robledo, Phys. Rev. C 77 (2008) 064322.
[6] R. Fossion, D. Bonatsos, G.A. Lalazissis, Phys. Rev. C 73 (2006) 044310.
[7] P.D. Stevenson, et al., Phys. Rev. C 72 (2005) 047303.
[8] K. Nomura, et al., Phys. Rev. 83 (2011) 054303.
[9] P.M. Walker, F.R. Xu, Phys. Rev. C 74 (2006) 067303.
[10] P.M. Walker, F.R. Xu, Phys. Lett. B 635 (2006) 286.
[11] Y.D. Fang, et al., Phys. Rev. C 83 (2011) 054323.
[12] T.R. Saitoh, et al., Phys. Scr. T88 (2000) 67.
[13] P.M. Walker, G.D. Dracoulis, Nature 399 (1999) 35.
[14] P.M. Walker, G.D. Dracoulis, Hyp. Int. 135 (2001) 83.
[15] T. Bengtsson, R.A. Brogia, E. Vogezzi, F. Barranco, F. Dönau, Jing-ye Zhang, Phys. Rev. Lett. 62 (1989) 2448.
[16] K. Narimutsu, Y.R. Shimizu, T. Shizuma, Nucl. Phys. A 601 (1996) 69.
[17] T. Shizuma, et al., Phys. Rev. C 65 (2002) 064310.
[18] G.A. Jones, et al., Acta Physica Polonica B 36 (2005) 1323.
[19] D. Mehta, et al., Z. Phys. A 339 (1991) 317.
[20] R. Broda, J. Phys. G 32 (2006) R151.
[21] R.V.F. Janssens, F.S. Stephens, Nucl. Phys. News 6 (1996) 9.
[22] G.J. Lane, et al., Phys. Rev. C 82 (2010) 051304(R).
[23] G.D. Dracoulis, et al., in: Proceedings of the Rutherford Centennial Conference on Nuclear Physics, UK, 8–12 August 2011, Journal of Physics: Conference Series (JPCS).
[24] G.D. Dracoulis, et al., in preparation.
[25] G.D. Dracoulis, et al., Phys. Rev. C 71 (2005) 044326.
[26] J. Lukasiak, R. Kaczarowski, J. Jastrzebski, S. Andre, J. Treherne, Nucl. Phys. A 313 (1979) 191.
[27] T. Kibédi, et al., Nucl. Instr. Meth. A 589 (2008) 202.
[28] P. Möller, J.R. Nix, W.D. Myers, W.J. Swiatecki, At. Data Nucl. Data Tables 59 (1995) 185.
[29] F.R. Xu, P.M. Walker, J.A. Sheikh, R. Wyss, Phys. Lett. B 435 (1998) 257.
[30] F.R. Xu, Chin. Phys. Lett. 18 (2001) 750.